

# MICROSTRUCTURAL ANALYSIS OF STAINLESS STEEL CLADDING DEPOSITED WITH PULSED CURRENT AND CONVENTIONAL CONTINUOUS CURRENT GMAW PROCESSES

**Marinho, Fábio Luis Castro**

Federal University of Pará, Department of Mechanic Engineering – Rua Augusto Corrêa, 01 – zip code: 66075-110, P.O.box: 479  
Belém – Pará – Brazil.

[marinho.ufpa@gmail.com](mailto:marinho.ufpa@gmail.com)

**Quintana, Frank Leslie Perez**

Federal University of Pará, Department of Mechanic Engineering – Belém – PA – Brazil.

[frankleslie@bol.com.br](mailto:frankleslie@bol.com.br)

**Filho, Cláudio Siqueira Alves**

Federal University of Pará, Department of Mechanic Engineering – Belém – PA – Brazil.

[siqueira@ufpa.br](mailto:siqueira@ufpa.br)

**Mota, Carlos Alberto Mendes da**

Federal University of Pará, Department of Mechanic Engineering – Belém – PA – Brazil.

[cmota@ufpa.br](mailto:cmota@ufpa.br)

**Braga, Eduardo de Magalhães**

Federal University of Pará, Department of Mechanic Engineering – Belém – PA – Brazil.

[edbraga@ufpa.br](mailto:edbraga@ufpa.br)

*Abstract. Stainless steel cladding was deposited on stainless steel plates using the pulsed current and conventional continuous current gas metal arc welding (GMAW) processes. Micrographs of three specified points were taken with the purpose of evaluating the solidification microstructure for both processes. The influence of mean current and pulse parameters on the secondary arm spacing was also verified, by comparing the values found for the continuous current to those found for the pulsed current GMAW process. It was observed through the micrographs that the pulsed current GMAW produced a microstructure with a finer aspect. It was also noticed two different ferrite morphologies (vermicular and lathy), which characterize primary ferrite solidification mode. This solidification mode attributes the cladding, among other properties, a high resistance to hot cracking. However, the secondary arm spacing revealed that for the same process, the refinement of the structure is largely affected by mean current.*

*Keywords: Solidification mode, Ferrite morphology, arm spacing, GMAW process*

## 1. INTRODUCTION

Solidification microstructure of metallic alloys has been a widely studied characteristic during the last decades, when advances in technology have made it possible to do a deeper investigation and better control on the parameters involved in this process. The microstructure of stainless steels to room temperature correspond to that predicted by the equilibrium diagram (Fig. 1), where it is noticed that different relations between chromium and nickel may result in ferrite ( $\alpha$ ) or austenite ( $\gamma$ ) as primary solidification phase, according to an increase or decrease in the content of these elements in alloy composition. However, during regular solidification processes, such as casting and welding, the resulting microstructure does not correspond to that predicted by the equilibrium diagram, due to high cooling rates observed in these conditions. In austenitic stainless steel alloys, particularly, the equilibrium diagram predicts a completely austenitic structure at the end of steady-state solidification. However, during a regular process, at least one second phase (ferrite) is present in the microstructure of these alloys. In the welding deposits, the microstructure is found to be governed by the welding characteristics, which largely affect the heat input. Such characteristics consist of the process, electrode polarity, diameter, current, pulse parameters (when pulsed current is used), plate thickness, etc.

Many authors in the scientific literature propose four main solidification modes (represented in Fig. 1). From these modes, the primary ferrite solidification (FA) is the one which has been most investigated by researchers at the present time. According to Padilha and Guedes (1994), such interest is due, among other reasons, to the minor susceptibility to hot cracking observed in alloys that solidify in this sequence, either in casting or welding processes. These writers attribute this characteristic to the presence of ferrite as the primary phase in this solidification mode. Bilmez and Gonzales (1995) state that the higher thermal conductivity and mass diffusion of centered face cubic (CFC) structure, present in the ferritic phase, make it possible for the formation of cellular dendrite morphology under solidification conditions typical of welding processes. Morphology, as well as the other characteristics of dendritic structures (i.e. spacing), have been used by researchers to evaluate, among other aspects, the mechanical and corrosive properties of metallic alloys. This paper focuses on the effect of mean current on the microstructural characteristics (morphology and secondary dendrite arm spacing) of weld claddings deposited using the GMAW (Gas Metal Arc Welding) process. The

influence of pulse parameters will also be evaluated, by comparing microstructures of welds performed using the conventional continuous current GMAW (CCC GMAW) to those with the pulsed current GMAW (PC GMAW) process.

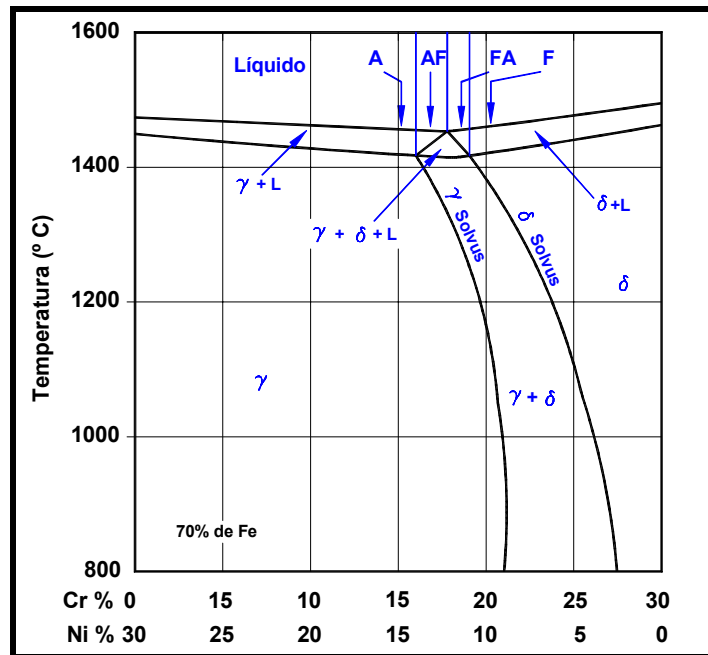


Figure 1 – Vertical section of a quasi-binary Fe-Cr-Ni diagram, for 70% of Fe in weight.

## 2. EXPERIMENTAL PROCEDURE

The cladding of a 5-mm thick stainless steel plate was performed with a 1.2-mm-diameter stainless steel filler metal, of specification AWS ER309L, and a 98%Ar + 2%O gas shielding at a flow rate of 15 l/min. Before the cladding, the base metal surface was mechanically cleaned, in order to avoid inclusion of contaminants. The GMAW gun was fixed in automatic traveling equipment, capable of moving in longitudinal direction at desired speed. The weld beads were superposed at 30%, fully covering the substrate (plates of UNS S30400 stainless steel). The cladding was deposited first with conventional continuous current, and later with pulsed current GMAW process. The weld parameters for the pulsed current GMAW were determined using the methodology proposed by Amin (1983). The relation between wire-feed speed ( $W_s$ ) and traveling speed ( $T_s$ ) remained constant and equaled to 10. The values for wire-feed speeds and traveling speeds, used to determine the welding parameters, are shown in Tab 1. From the seven levels presented in Tab. 1, levels 2, 4 and 6 (which produced better stability) were chosen to be used in this work. Each experiment was repeated three times, so that the consistency of the results could be verified. The welding parameters, such as mean current ( $I_m$ ), peak current ( $I_p$ ), base current ( $I_b$ ), pulse frequency ( $f$ ) and pulse duration ( $t_p$ ) are available in Tab. 2.

Table 1 – Values for wire-feed speed and traveling speed used to determine the pulse parameters

Níveis	1	2	3	4	5	6	7
Wire-feed Speed - $W_s$ (m/min)	5.0	7.0	8.0	8.5	9.0	9.5	10.0
Travelling Speed (cm/min)	50	70	80	85	90	95	100

Table 2 – Welding Parameters

$W_s$ (m/min)	$I_m$ (A)	$I_p$ (A)	$I_b$ (A)	F (Hz)	$t_p$ (ms)	Arc Voltage (V)
7.0	165	-	-	0	-	26
7.0	165	203	145	173	2,0	26
8.5	175	-	-	0	-	26
8.5	175	203	160	173	2,0	26
9.5	185	-	-	0	-	26
9.5	185	203	176	173	2,0	26

For microstructural analyses, specimens were collected at 20 mm up from the beginning of the cladding. The transverse section of the cladding, showed in Fig. 2, was prepared by standard metallographic procedure and etched with a solution containing 10% nitric acid, 10% acetic acid, 15% hydrochloric acid and 5% glycerol. The points analyzed in the cross section of the specimens are schematically represented in Fig. 2. Metallographic studies were carried out under an optical microscope Q500 MC – Leyca Cambridge. Dendrite arm spacing measurement was performed in accordance with the methodology proposed by Gündüz (2002).

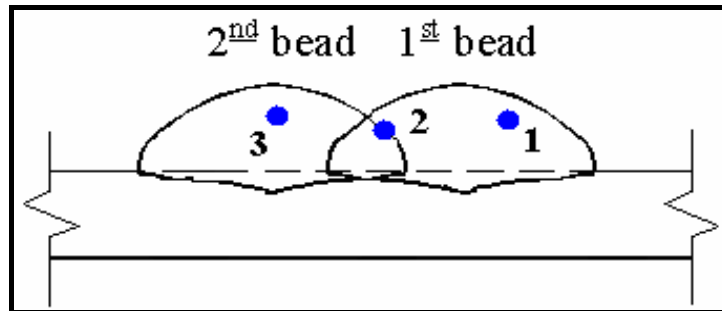


Figure 2 – Points on transverse section from where the analyzed micrographs were taken.

### 3. RESULTS AND DISCUSSION

#### 3.1. Microstructure characterization

An important characteristic observed in the microstructure of the cladding was the changing in ferrite morphology at the interface between two consecutive beads (point 2 in Fig. 2). Figures 3 and 4 show that a finer vermicular dendrite structure seems to form in the first bead deposited, while some lathy morphology can be observed forming from the interface to the center of the second bead.

It is noticed through Figs. 5 and 6 (point 3) separately, that the increment in mean current resulted in an apparent coarsening of the columnar dendritic growth. This observation is in agreement with the results found by Gosh et al (1998), working on stainless steel cladding deposited through the GMAW process. By this time, Gosh observed that by increasing the mean current, the hardness of the cladding is reduced. This observation may be related to a possible coarsening in microstructure as the mean current is increased, since it is known that the hardness is reduced as the grain becomes coarser. The use of higher mean currents results in a longer time for the ferrite formation, increasing the content of this phase (Braga, 2002). By comparing Figs. 5 and 6, it is observed that the use of continuous current resulted in a more directional dendritic growth, with longer primary arm lengths. This directionality (which is more evident for the higher level of current), might probably be caused by the flux of heat extracted by the first bead.

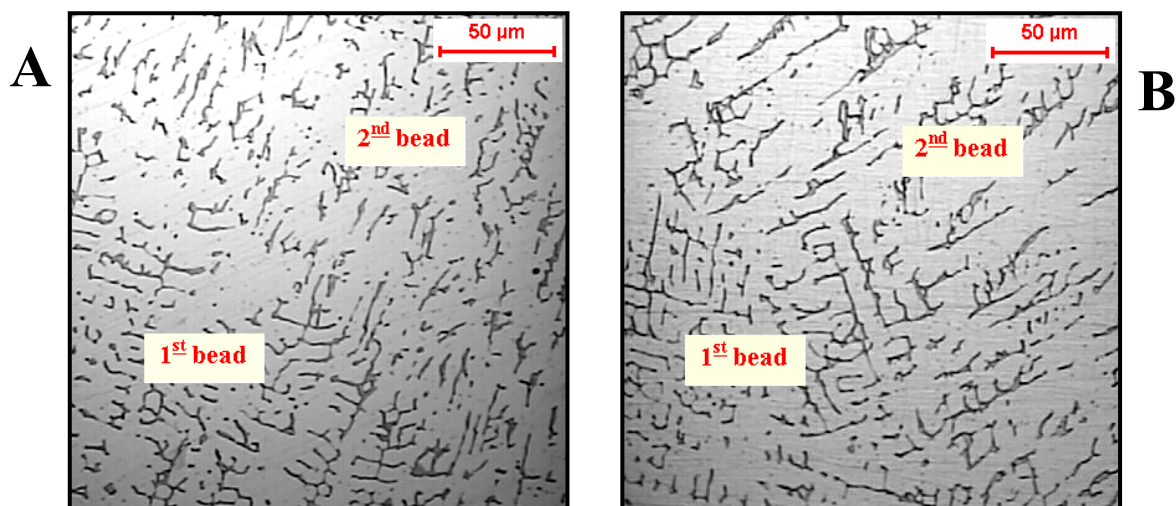


Figure 3 – Micrographs taken from point 2 (refer to Fig. 2) of the continuous current GMAW cladding. A)  $W_s = 7.0$  m/min,  $I_m = 165$  A; B)  $W_s = 9.5$  m/min,  $I_m = 185$  A – magnitude 500x

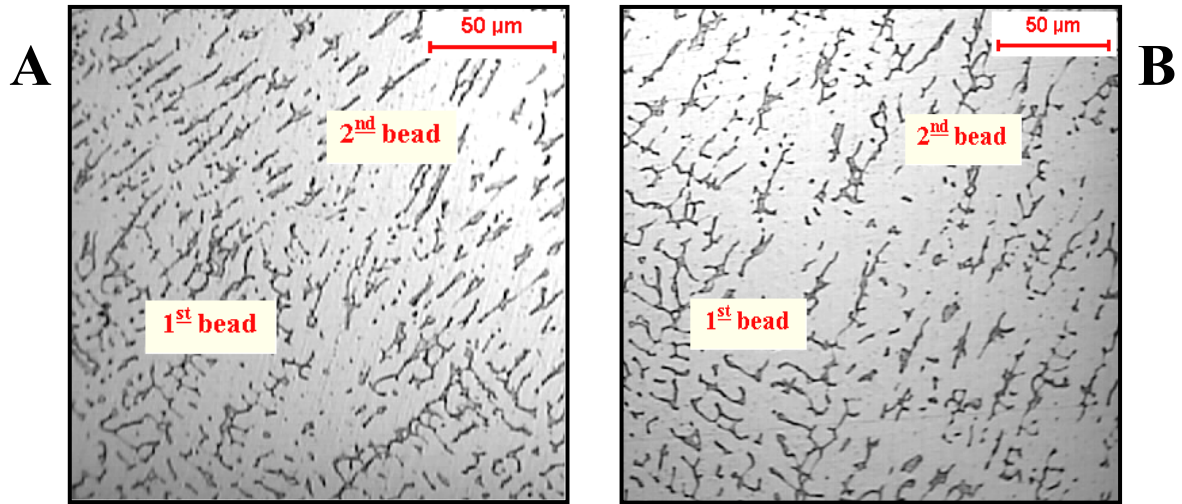


Figure 4 – Micrographs taken from point 2 of the pulsed current GMAW cladding. A)  $W_s = 7.0$  m/min,  $I_m = 165$  A; B)  $W_s = 9.5$  m/min,  $I_m = 185$  A – magnitude 500x

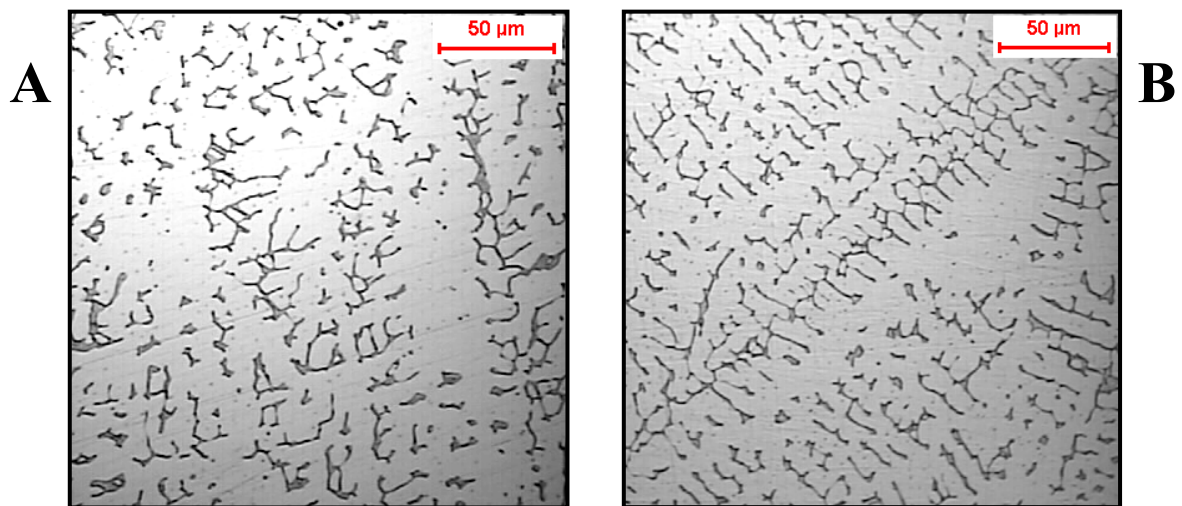


Figure 5 – Micrographs taken from point 3 of the continuous current GMAW cladding. A)  $W_s = 7.0$  m/min,  $I_m = 165$  A; B)  $W_s = 9.5$  m/min,  $I_m = 185$  A – magnitude 500x

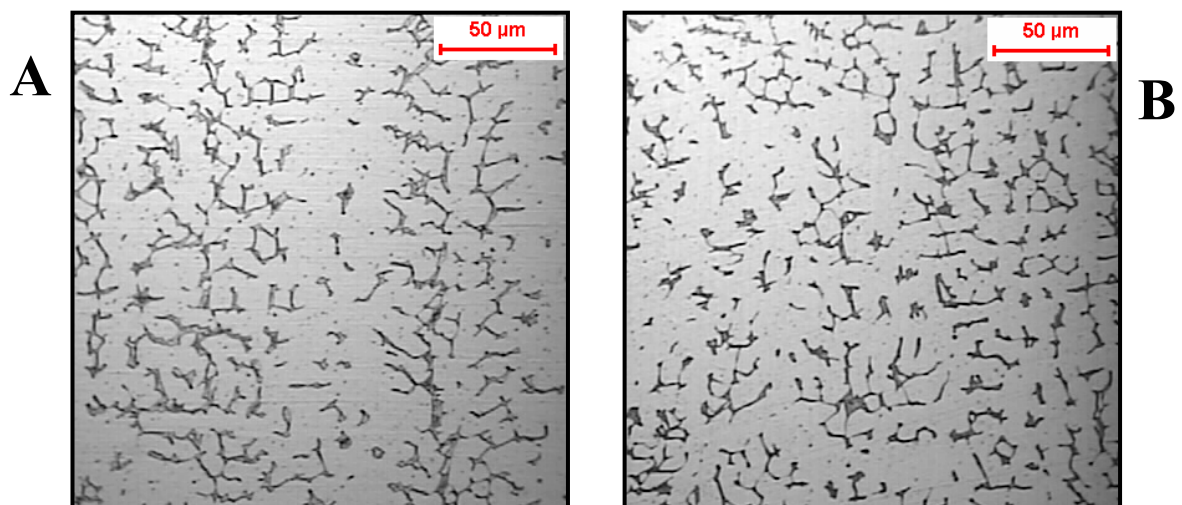


Figure 6 – Micrographs taken from point 3 of the pulsed current GMAW cladding. A)  $W_s = 7.0$  m/min,  $I_m = 165$  A; B)  $W_s = 9.5$  m/min,  $I_m = 185$  A – magnitude 500x



Figures 7 and 8 show the microstructural aspect of the cladding at point 1 (Fig. 2). Through these Figures, a refinement of the solidification microstructure can be observed, as the process is changed from continuous current to pulsed current GMAW.

In all micrographs, the structure is basically formed by austenite (white) and ferrite (black). The vermicular and lathy morphologies (identified in this work) are signs of primary ferrite solidification mode (Bilmes and Gonz  les, 1995).

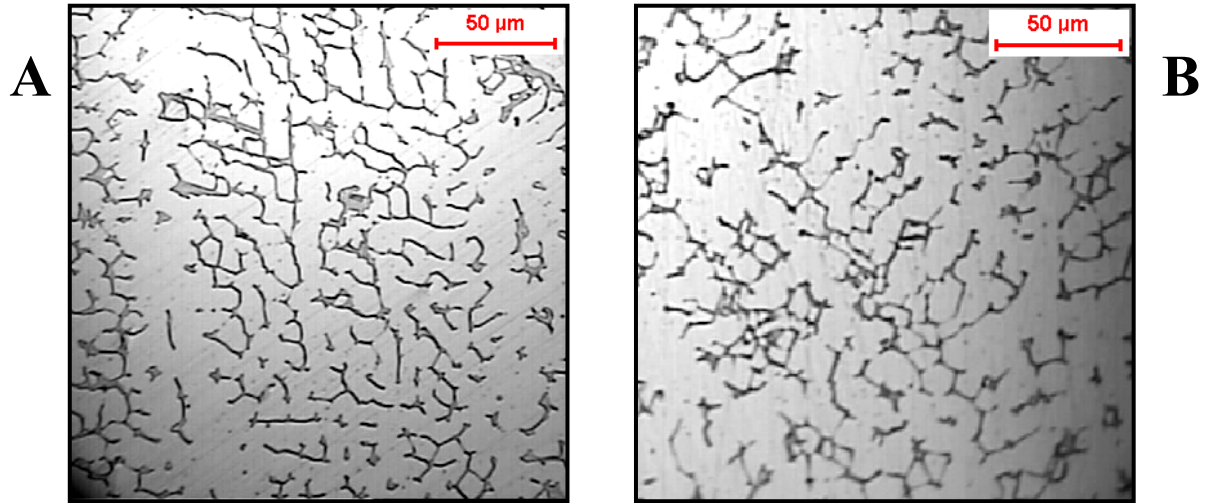


Figure 7 – Micrographs taken from point 1 of the continuous current GMAW cladding. A)  $W_s = 7.0$  m/min,  $I_m = 165$  A; B)  $W_s = 9.5$  m/min,  $I_m = 185$  A – magnitude 500x

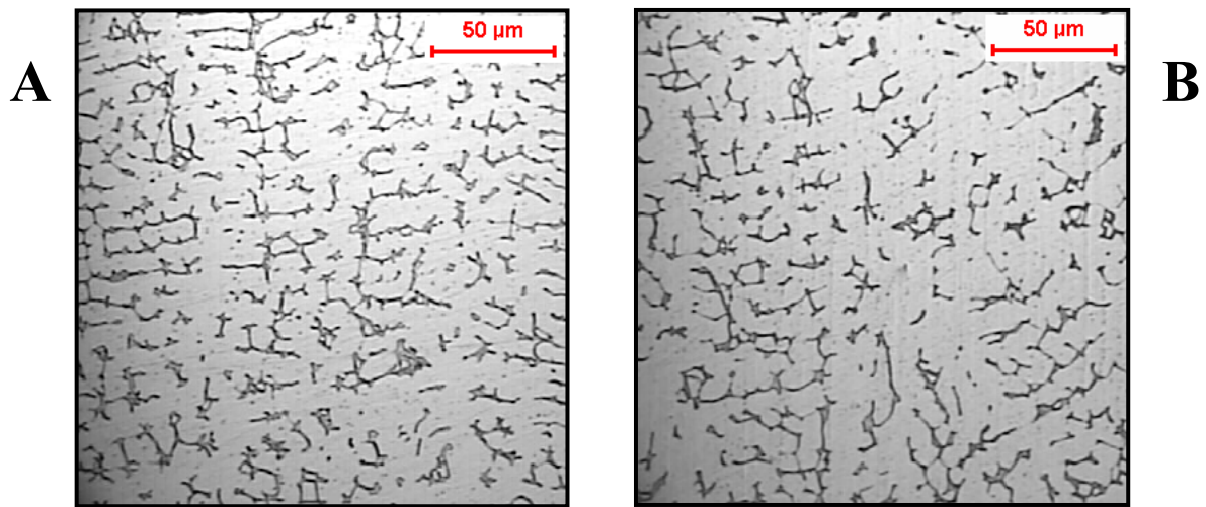


Figure 8 – Micrographs taken from point 1 of the pulsed current GMAW cladding. A)  $W_s = 7.0$  m/min,  $I_m = 165$  A; B)  $W_s = 9.5$  m/min,  $I_m = 185$  A – magnitude 500x

### 3.2. Dendrite secondary arm spacing ( $\lambda_2$ )

In order to evaluate the effect of process and mean current, a variance analysis was done on the values measured for the secondary arm spacing. According to Table 3, the mean current affected  $\lambda_2$  at all the analyzed points, while the process did not influence this parameter at any point. Figure 9 shows the  $\lambda_2$  behavior (as a response to the mean current) at point 3. It is noticed that the secondary spacing is increased as mean current is incremented, characterizing a coarsening in the solidification microstructure. However, this behavior was more regular with the pulsed current than with the continuous current GMAW process. Since the same behavior was observed at the points 1 and 2, Fig. 10 can also be representative of these points.

An average value of  $\lambda_2$  for the three levels of mean current was determined at each point, so that the behavior of  $\lambda_2$  at the different points could be evaluated independently on the variation in mean current. Table 4 shows that the deviation in  $\lambda_2$  values, comparing the different processes, is more significant at point 1. Through Figure 10, it can be

observed that the spacing was significantly reduced at the points 2 and 3, compared to the values found at point 1. This decrease can be attributed to the additional heat extraction caused by the first bead, which resulted in a higher solidification velocity in the second bead deposited. It is also observed through Fig. 10 that  $\lambda_2$  is smaller for the PC GMAW at all points, thus characterizing a more refined microstructure for this process.

Table 3 – Results for the variance analysis on  $\lambda_2$

Factor	Level of significance (%)		
	Point 1	Point 2	Point 3
Process	10.3	14.6	34.3
Mean current	<b>0.00*</b>	<b>0.00*</b>	<b>0.000*</b>
Interaction (Im x Process)	<b>0.00*</b>	<b>0.00*</b>	<b>0.000*</b>

Note: significance index ( $\alpha$ ) = 5%.

Table 4 – Average values for  $\lambda_2$  at each point

Point	Secondary arm spacing ( $\mu\text{m}$ )		
	CCC GMAW	PC GMAW	Deviation (%)
1	$11.51 \pm 0.50$	$10.34 \pm 0.55$	10.2
2	$8.45 \pm 0.47$	$8.32 \pm 0.43$	1.54
3	$8.31 \pm 0.64$	$8.22 \pm 0.55$	1.1

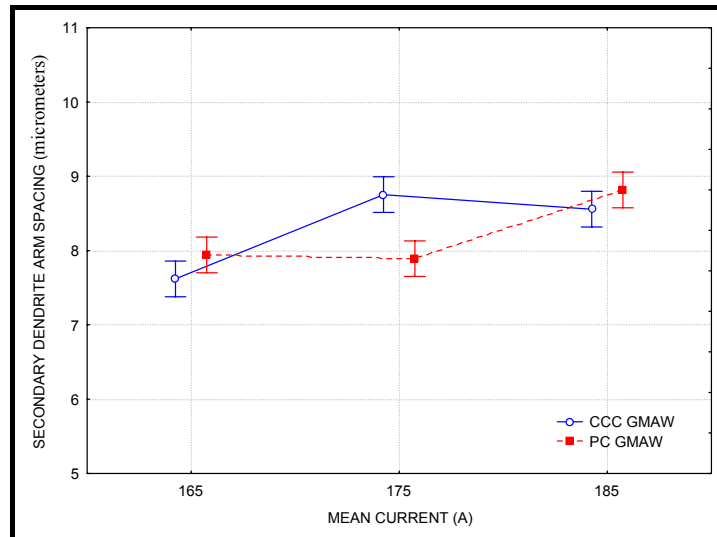


Figure 9 – Effect of mean current on the secondary arm spacing at point 3.

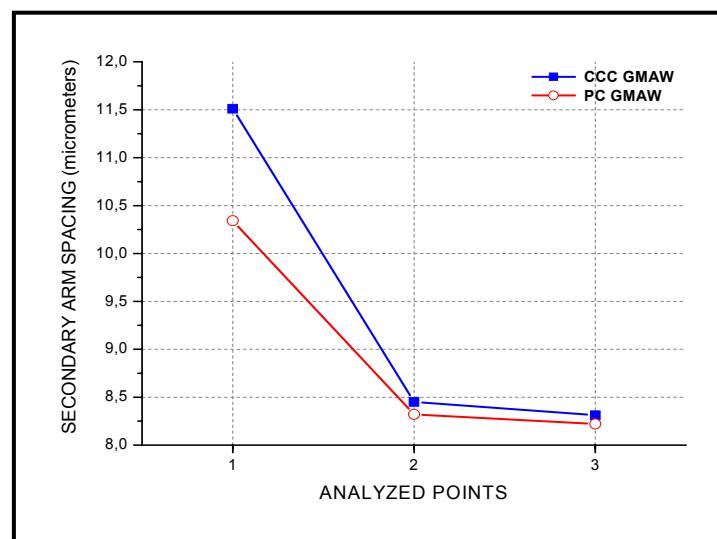


Figure 10 - Variation in  $\lambda_2$  according to the point analyzed.

#### 4. Conclusions

Through the ferrite morphologies (vermicular and lathy) observed in the cladding, it can be concluded that independently on the welding parameters, the solidification mode is primary ferrite (FA). This characteristic gives the cladding a minor susceptibility to hot cracking, which is a desirable property for welded structures. This property has a special importance when such structure is subjected to a thermal cycle (i.e. oil refinery towers).

According to the secondary dendrite arm spacing values, the use of pulsed current GMAW in stainless steel cladding of stainless steel was more beneficial over the use of conventional continuous current, since this process produced a comparatively finer microstructure. However, for the same process the secondary arm spacing was largely affected by mean current.

#### 5. Acknowledgements

Thanks are due to UFPA (Federal University of Pará - Brazil), for the laboratorial infrastructure and to Cnpq (Brazilian Council of Scientific and Technologic Development), for the financial support.

#### 6. References

- Amin, M., "Pulse Current Parameters for Arc Stability and Controlled Metal Transfer in Arc Welding". Metal Construction, v. 15, n. 5, p. 272-278, May 1983.
- Bilmes, P., González, A., Llorente, C. and Solari, M., "Influencia de la Morfología de solidificación de la Ferrita  $\delta$  del Metal de Soldadura de Aceros Inoxidables Austeníticos Sobre las Propiedades de la Unión". Consejo Nacional de Investigaciones Científicas e Técnicas, Facultad de Ingeniería. Universidad Nacional de la Plata, Argentina. p. 127-141, Diciembre 1995.
- Braga, E. M., "Efeito do Nitrogênio nas Trincas de Solidificação em Soldas de Aço Austenítico". Doctor's degree thesis, Faculdade de Engenharia Mecânica, Universidade Estadual de Campinas, São Paulo (Brasil) 2002.
- Ghosh, P. K., Gupta P. C., Goyal, V. K., "Stainless Steel Cladding of Structural Steel Plate Using the Pulsed Current GMAW Process". Welding Research Supplement, India, p. 307s-314s, July 1998.
- Gunduz M.<sup>1</sup>; Cadirli E., "Directional solidification of aluminium-copper alloys". Materials Science and Engineering: A, 30 April 2002, vol. 327, no. 2, pp. 167-185(19).
- Padilha, A. F., Guedes, L. C. "Aços Inoxidáveis Austeníticos" Hemus Publishing Company, São Paulo (Brasil) 1994.

#### 7. Responsibility notice

The authors are the only responsible for the printed material included in this paper.